Clays and Clay Minerals, Vol. 68, No. 1:50–66, 2020

TRACE AND RARE EARTH ELEMENT DISTRIBUTION AND MOBILITY DURING DIAGENETIC ALTERATION OF VOLCANIC ASH TO BENTONITE IN EASTERN IRANIAN BENTONITE DEPOSITS

Alireza Namayandeh[1,2], Soroush Modabberi[2]*, and Alberto López-Galindo[3]

[1]Department of Geosciences, Virginia Tech, Blacksburg, VA 24061, USA
[2]School of Geology, College of Science, University of Tehran, Enghelab Avenue, P.O. Box 14155-6455, Tehran, Iran
[3]Instituto Andaluz de Ciencias de la Tierra (CSIC-Universidad de Granada), Avda. de las Palmeras, 4, 18100 Armilla, Granada, Spain

Abstract—The chemical composition of the source magma along with the physiochemical conditions of the depositional environment are the main controlling factors in determining the behavior and mobility of trace elements and rare earth elements (REEs) during the transformation of volcanic ash to bentonite. The purpose of the present study was to determine the distribution pattern and mobility of trace elements and REEs in several bentonite deposits formed by diagenetic alteration of volcanic ash in shallow alkaline water in eastern Iran. Using geochemical and statistical data, the degree of weathering in the parent rocks and the distribution and mobility of trace elements and REEs during the alteration process at seven deposits (Chah-Taleb, Chah-Keshmir, Chah-Golestan, Chah-Pirouz, Gholeh-Gelia, Kharman-Sar, and Khal-Kooh) were studied. None of the parent rocks showed an advanced degree of depositional reworking and, therefore, their chemical composition is representative of the volcanic ash from which the bentonites were formed. In the chondrite-normalized REE patterns of both parent rocks and bentonites, the light rare earth elements (LREEs) were found to be enriched relative to the heavy rare earth elements (HREEs). The variation in δEu and δCe values suggested a high-temperature (<200°C), suboxic, aquatic environment in which the conversion of volcanic ash to bentonite occurred. In the bivariate correlation analysis, Si showed a strong inverse relationship with Al and LREEs, while large ion lithophile elements (LILEs), high field strength elements (HFSEs), HREEs, and LREEs displayed a positive correlation between the elements of their respective groups. The R^2 values in the binary diagram of potential immobile elements against Al suggest a qualitative classification in which Ti, Gd, Ga, Pr, Tb, Nd, Sm, Ce, and Nb are considered immobile, and U, Dy, In, Sc, Hf, Zr, La, and Eu are considered to have had poor mobility during formation of the Eastern Iranian bentonite deposits.

Key Words—Diagenetic alteration · Eastern Iranian bentonites · Mobility · Rare earth elements · Trace elements · Volcanic ash

INTRODUCTION

The comparative chemistry of volcanic rocks before and after weathering is a key factor in the study of the source magma, the style of volcanic eruption, and tectonic processes in volcanic areas (Irvine & Baragar 1971; Winchester & Floyd 1976, 1977; Pearce et al. 1984; Christidis 1998; Batchelor & Evans 2000; Yusoff et al. 2013; Huff et al. 2014; Kiipli et al. 2014, 2017; Xing et al. 2015; Modabberi et al. 2019). Moreover, studies on the concentration of trace and rare earth elements (REEs) in volcanic rocks, and particularly their alteration products in sedimentary environments, such as bentonite, are of particular interest and have been addressed by several researchers (Roberts & Merriman 1990; Batchelor & Evans 2000; Christidis 2001; Foreman et al. 2008; Inanli et al. 2009; Yildiz & Dumlupunar 2009; Hetherington et al. 2011; Batchelor 2014; Kiipli et al. 2014, 2017; Caballero & de Cisneros 2017; Kadir et al. 2017; Elliott et al. 2018).

Immobile elements are proper proxies of the source magma because their concentration will remain unchanged during the alteration of volcanic rocks to bentonite, whereas mobile elements provide insight into the diagenetic processes forming bentonite deposits (Christidis 1998; Özdamar et al. 2014; Kiipli et al. 2017). In sedimentary environments where volcanic rocks undergo alteration, the mobility of elements is controlled by processes commonly involved in mineral–water interface interactions such as sorption/desorption, dissolution/precipitation, and oxidation/reduction (Brantley 2008; Chorover & Brusseau 2008; Rimstidt 2014; Schaefer et al. 2017; Namayandeh & Kabengi 2019). The study of the mobility of elements during the alteration of volcanic rocks, therefore, sheds light on the nature of the environment in which bentonite is formed.

Because bentonite occurs in various sedimentary environments, a consistent behavior among elements during the alteration is hardly to be expected, so labeling each element as either mobile or immobile for all circumstances is, therefore, inappropriate. Several studies on the mobility of elements during the alteration of volcanic rocks have considered a broad range of elements (from Al, Ti, Zr, and REEs to Sc, Th, Hf, Ta, Fe, Co, Sb, U, Co, Cr, and Ga) to be immobile (Winchester & Floyd 1977; Pearce et al. 1984; Zielinski 1985; Huff et al. 1989; Christidis 1998; Zhou et al. 2000; Inanli et al. 2009; Dai

Electronic supplementary material The online version of this article (https://doi.org/10.1007/s42860-019-00054-9) contains supplementary material, which is available to authorized users.

* E-mail address of corresponding author: modabberi@ut.ac.ir
DOI: 10.1007/s42860-019-00054-9

https://doi.org/10.1007/s42860-019-00054-9 Published online by Cambridge University Press

et al. 2011; Batchelor 2014; Kiipli et al. 2014), whereas McHenry (2009) reported that Ti and Zr showed significant mobility during closed-basin saline–alkaline tephra alteration and, by examining the chemical composition of three altered volcanic ash layers, Kiipli et al. (2017) reported that Al, Cd, Ta, Hf, and Th showed small-scale mobility during the conversion of volcanic ash, while in layers with thicknesses <1 cm, Sc, V, Ga, Y, and REEs were significantly mobile. Nb, commonly considered an immobile element, was found to be mobile by Siir et al. (2015) up to a few centimeters from the parent rock, emphasizing the fact that the geochemical conditions of sedimentary environments such as pH, salinity, temperature, water/rock ratio, and redox conditions govern the mobility of elements during volcanic ash alteration (Bau 1991; Chen et al. 2015; Liao et al. 2016; Hong et al. 2019).

The objective of the present research was to determine the distribution pattern and mobility of trace elements and REEs during the transformation of volcanic ash to bentonite in the eastern Iranian bentonite deposits. The behavior of trace elements and REEs are hypothesized to be controlled by the chemical composition of the source magma that formed the parent rocks and the physiochemical conditions of the local environment in which the bentonites were formed. Two papers studying the industrial applications (Modabberi et al. 2015) and genesis (Modabberi et al. 2019) of the eastern Iranian bentonites are believed to be the first research on the chemistry of trace elements and REEs during bentonite formation in this study area, so the present research was designed to augment those studies.

GEOLOGICAL SETTING

The eastern Iranian bentonite deposits are located in the Lut structural zone, close to Sarayan and Ferdows towns and also around Birjand in South Khorasan province. The study area has been influenced significantly by Eocene-Oligo-Miocene magmatism and is made up of basaltic to rhyolitic volcanic and sub-volcanic rocks (Stocklin 1968; Berberian & King 1981; Pang et al. 2012, 2013).

The geological setting, morphology, and the mineralogical and lithological properties of the eastern Iranian bentonite deposits were described by Modabberi et al. (2019) and the same set of groups provided in that paper is used here (Table 1, see Section A of the Supplementary Information for the simplified geological map of the study area). To determine the tectonic setting, source magma composition, and their magmatic series, several geochemical diagrams such as Nb/Y vs Zr/Ti (Winchester & Floyd 1977), Ta/Yb, Y/Nb (Pearce et al. 1984), SiO_2 vs $Na_2 + K_2O$, and AFM (Irvine & Baragar 1971) were used by Modabberi et al. (2019). The results showed that the parent rocks of the bentonite deposits in eastern Iran were formed in a subduction zone, and their magma sources were found to be mostly acidic in composition, having a calc-alkaline affinity. Based on the X-ray powder diffractometry (XRPD) conducted as part of this research, the main mineralogical phases among the bentonite samples were secondary Na-montmorillonite and opaline silica, with lesser amounts of quartz, feldspars, carbonates, halite, and illite (Table 1). Modabberi et al. (2019) also suggested a diagenetic alteration in an aqueous environment with low water/rock ratios, such as a lagoon for the formation of the bentonite deposits, which was evidenced by the large amount of opaline silica and lack of zeolites in the bentonite samples.

In all the deposits studied, the parent rocks are in contact with the top of the bentonite layer(s) and in some deposits, a gradual transition from the parent rocks to the bentonites with strata-bound geometry is clearly observed (Fig. 1). In the Chah-Taleb (ST), Chah-Keshmir (SK), Chah-Pirouz (SP), and Chah-Golestan (SG) located in Sarayan, the parent rocks consist predominantly of volcanic ash shards and plagioclase, chalcedony, and calcite. In Kharman-Sar (FKH) and Gholeh-Gelia (FGH), close to the town of Ferdows, the parent rocks were found to be a volcanic sandstone containing quartz, biotite, plagioclase, and Fe oxides. In the Khal-Kooh (FKHS) deposit, the parent rock consists of both volcanic ash shards and volcanic sandstone (Modabberi et al. 2019).

MATERIALS AND METHODS

Several samples of bentonites and parent rocks were taken along vertical profiles of the bentonite deposit layers from active mines at seven deposits situated in South Khorasan (eastern Iran). In the Chah-Taleb (ST), Chah-Keshmir (SK), Chah-Pirouz (SP), Gholeh-Gelia (FGH), and Kharman-Sar (FKH), only one bed of bentonite was found and it had strata-bound geometry and its parent rock was exposed to the surface, whereas in Chah-Golestan (SG) and Khal-Kooh (FKHS) more alternating beds of bentonites were found at the surface.

Samples of up to 1 kg in weight were collected from the deposits and ground to <20 μm and oven-dried at 65°C.

To determine the major element concentrations, X-ray fluorescence (XRF) analyses were carried out using a commercial wavelength dispersive X-ray fluorescence instrument (Bruker AXS-S4 Pioneer made in Karlsruhe, Germany, installed in Instituto Andaluz de Ciencias de la Tierra (CSIC-Universidad de Granada)) equipped with a Rh anode X-ray tube (60 kV, 150 mA), three analyzer crystals (OVO-55, LiF 200, and PET), and a flow proportional counter for light element detection and a scintillation counter for heavy elements. The fundamental parameters method using software linked to the equipment was utilized to quantify the elemental compositions of bulk samples. The samples were ground to fine powders using an agate pestle and mortar, and 5 g of each sample was then mixed and homogenized with 0.5 g of a binder (Hoechst wax C micropowder). Using a small aluminum sample holder ~4 cm in diameter, an XRF pellet was produced and pressed for 30 s at 90 bar in a Nannetti hydraulic press. Loss on ignition (LOI) was determined from the weight difference between samples heated at 105°C overnight and then heated at 900°C for 1 h. Accuracy was in the 1–2% range, and precision was < 0.3%, depending on the major element.

Inductively coupled plasma-mass spectrometry (ICP-MS) analyses were conducted at AMDEL Ltd. (Bureau

https://doi.org/10.1007/s42860-019-00054-9 Published online by Cambridge University Press

Table 1 Mineralogical and lithological properties of the eastern Iranian bentonite deposits (Modabberi et al. 2019).

Deposits		Smectite content %	Opaline silica content %	Source magma composition	Tectonic setting	Magmatic series	Origin environment
Group 1	ST	71	26	Trachytic to trachy-andesitic	Subduction zone	Calc-alkaline	Shallow aqueous environment
	SK	65	34	Trachy-andesitic		Calc-alkaline	
Group 2	SG[1]	57	38	Rhyolitic to rhyodacitic		Calc-alkaline	
	SP	60	39	Rhyolitic to rhyodacitic		Calc-alkaline	
Group 3	FGH	70	25	Rhyodacitic-dacitic		Calc-alkaline	
	FKH	68	11	Trachy-andesite		Tholeiitic	
Group 4	FKHS	61	32	Rhyodacitic-dacitic		Calc-alkaline	

[1] Seven samples were taken from SG deposit. The sample shown here is that (SG-G) which was in contact with the parent rock. See Modabberi et al. (2019) for detailed information about the mineralogical and lithological properties of the other samples.

Veritas), Australia, to determine trace and REE elements of the samples. Accuracy was in the 1–3% range, depending on the element amount. Two spider diagrams were used to study losses/gains and distribution of trace elements and REEs in the conversion of volcanic ash to bentonite. In the first diagram, REE concentrations of both bentonites and parent rocks were normalized to the concentration of chondrite meteorites, and in the second one, trace elements and REE contents of the bentonites were normalized to the respective parent rocks to assess the degree to which elements were lost or gained. Using *SPSS Statistics* version 25 package (SPSS Inc., Chicago, Illinois, USA), a bivariate correlation analysis was carried out on all elements to determine the relationship between elements during transformation of the volcanic ash. Binary diagrams of Al against various elements were used to determine the mobility of elements. In the binary diagrams, the samples from a single deposit (SG) were used to decrease the impact of local geochemical and lithological conditions such as slight variation in pH, salinity, temperature, and water/rock ratio in the aqueous environment in which bentonites were formed.

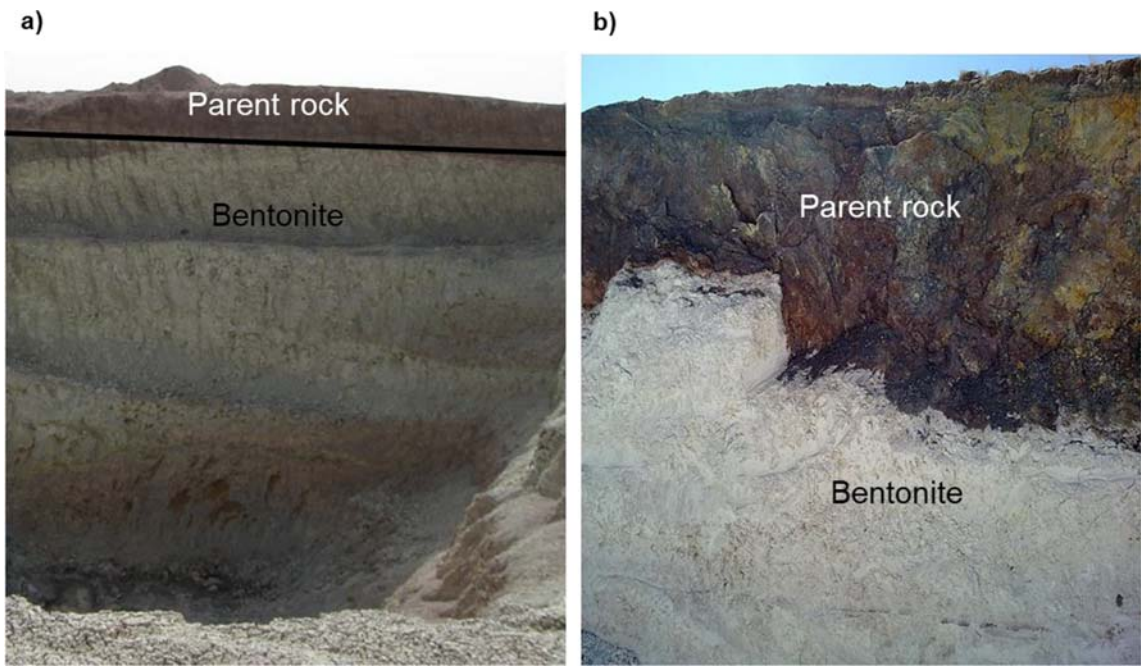

Fig. 1. Representative pictures of the morphology of bentonites and parent rocks in **a** Khal-Kooh and **b** Chah-Taleb deposits.

https://doi.org/10.1007/s42860-019-00054-9 Published online by Cambridge University Press

RESULTS AND DISCUSSION

Degree of Weathering in the Parent Rocks

The major, trace, and rare earth elements contents of the studied parent rocks and bentonites were given by Modabberi *et al.* (2019, see Section B of the SI).

Evaluating the degree of weathering of the parent rocks is essential to study the mobility of elements during the alteration of volcanic ash to bentonite because knowing whether their chemical composition is an accurate reflection of the volcanic ash from which the bentonites were formed is imperative. TiO_2/Al_2O_3 ratios of felsic volcanic ash have been used widely to determine the chemistry of source magma and the intensity of physical reworking and chemical alteration of igneous rocks (Spears & Kanaris-Sotiriou 1979; Zhou & Kyte 1988; Hayashi et al. 1997; Burger et al. 2002; Hints et al. 2008; He et al. 2014; Dai et al. 2017; Hong et al. 2019). Despite the ongoing discussions regarding the degree of Al and Ti mobility, they have consistently been found to be the most chemically immobile constituents during volcanic ash devitrification to authigenic bentonite (Nesbitt 1979; Slack & Stevens 1994; Laviano & Mongelli 1996; Hong et al. 2019). The mobility of Al and Ti are not exactly similar, and Ti is relatively more mobile than Al (Nesbitt 1979; Arslan et al. 2010; Hong et al. 2019), causing the TiO_2/Al_2O_3 ratio to diminish progressively with increasing intensity of chemical and physical weathering. For felsic volcanic rocks, Hong et al. (2019) allocated TiO_2/Al_2O_3 values of <0.055 to primary ash compositions, values of 0.055–0.140 to moderate secondary overprints, and values of >0.140 to strong secondary overprints.

Based on the Nb/Y vs Zr/Ti diagram (Winchester & Floyd 1977) created by Modabberi et al. (2019), the source magma for the parent rocks was reported to be mostly acidic. Also, the magma series of most of the samples were found to be calc-alkaline (Table 1); therefore, the TiO_2/Al_2O_3 ratio can be used to evaluate the degree of weathering in the parent rocks. In the samples studied and with the exception of FKH, the TiO_2/Al_2O_3 values of the parent rocks are values of ≤0.055 (Table 2), thus representing weakly reworked tuffs with little weathering. The magmatic series of the FKH sample has a tholeiitic composition and its TiO_2/Al_2O_3 ratio is possibly related to the original rock composition rather than the degree of weathering (Table 1).

The δEu ratio is commonly considered to be an indicator of the source magma composition, not influenced by depositional reworking mechanisms (Zielinski 1982; Sverjensky 1984; McLennan 1989). The δEu ratio was calculated using the following formula (Liao et al. 2016):

$$\delta Eu = Eu_N/(Sm_N \times Gd_N)^{1/2} \quad (1)$$

where N denotes chondrite-normalized.

The TiO_2/Al_2O_3 vs δEu diagram was used to evaluate depositional reworking effects (Hong et al. 2019). Most of the samples fall in the zone of primary felsic tuffs, near the rhyolitic composition and, less significantly, andesite rock spots in the diagram. FKH is the only sample which falls in the field of weakly reworked tuffs (Fig. 2).

In addition, the Mineralogical Index of Alteration (MIA) was used to estimate the degree of mineralogical weathering (Voicu & Bardoux 2002; Yusoff et al. 2013):

$$MIA = 2 \times \left[\frac{Al_2O_3 \times 100}{(Al_2O_3 + CaO + Na_2O + K_2O)} - 50\right] \quad (2)$$

MIA values <20% were proposed to be indicative of incipient, 20–40% of weak, 40–60% of moderate, and 60–100% of intense to extreme weathering (Voicu & Bardoux 2002). The MIA values for parent rocks in Groups 1, 2, and 4 (see Modabberi *et al.* 2019 for groupings) are lower than or very close to 20% (none of the samples displayed an advanced degree of depositional reworking), while those of Group 3 (FKH and FGH) are higher (~35.0%) and fall within the weak weathering range (Table 2). These last two samples were formed predominantly from volcanic sandstone, and unlike samples of other groups, especially those around the town of Sarayan (Groups 1 and 2), no volcanic ash shards were observed. Some evidence of sedimentary-diagenetic processes was found, however, suggesting light reworking effects (Modabberi et al. 2019).

Based on the field observations and because the degree of weathering was weak, even in Group 3 samples, the parent rocks are considered to be accurate representatives of the original composition of the parental volcanic ash.

REEs and Trace Elements Distribution

LREEs vs HREEs REE fractionation provides useful insight into the composition of the source magma (Christidis 1998; Kiipli et al. 2017; Hong et al. 2019), the mineralogical and geochemical characteristics of the altered volcanic ash, and the environmental conditions of the alteration process (Bau 1991; MacRae et al. 1992; Nath et al. 1997; Chen et al. 2015; Liao et al. 2016). REE fractionation during the formation of diagenetic bentonites consists of two phases. In the first phase, some REEs, such as Eu and HREEs, are co-precipitated with plagioclases and/or incorporated into the structure of plagioclases in early-stage magma, causing their depletion in intermediate to felsic magma. The second phase of REE fractionation may occur after the deposition of volcanic ash in an aqueous environment where it undergoes alteration. The fractionation of REEs in the second phase is controlled by the pH, temperature, alkalinity, salinity, redox condition, and water/rock ratio in the aqueous environment (dos Muchangos 2006; He et al. 2014; Chen et al. 2015; Hong et al. 2019). This will be discussed more in the next sections.

The ΣLREE/ΣHREE ratio in the parent rocks varies from 6.29 to 8.97 (mean 7.69, Table 2). Similarly, the ΣLREE/ΣHREE ratio in bentonites showed a somewhat comparable variation, ranging from 6.90 to 8.54 (mean 7.67), indicating the relatively elevated concentration of LREEs in both parent rocks and bentonites.

The chondrite-normalized REE patterns of the parent rocks (P/C) and bentonites (B/C) suggest the same trend of LREEs enrichment relative to HREEs (Fig. 3).

https://doi.org/10.1007/s42860-019-00054-9 Published online by Cambridge University Press

Table 2 Weathering indices, ΣLREE/ΣHREE, δEu, and δCe values.

	Parent rock			Bentonite	Parent rock/ Chondrite		Bentonite/ Chondrite		Bentonite/ Parent rock	
	TiO_2/Al_2O_3	MIA[1]	ΣLREE/ΣHREE	ΣLREE/ΣHREE	δEu[2]	δCe[3]	δEu	δCe	δEu	δCe
ST	0.055	18.2	7.75	7.47	0.873	0.691	0.291	0.711	0.333	1.03
SK	0.023	16.4	6.90	6.90	0.741	0.961	0.741	0.961	0.359	1.17
SG	0.020	15.3	6.98	8.40	0.635	0.960	0.385	0.953	0.605	1.00
SP	0.021	21.5	6.29	7.52	0.635	0.982	0.393	0.991	0.606	0.948
FGH	0.045	35.2	8.97	7.35	0.732	0.977	0.399	0.972	0.545	0.925
FKH	0.067	34.0	8.66	7.53	0.902	1.01	0.750	0.966	0.831	0.950
FKHS	0.031	10.9	8.27	8.54	0.747	0.937	0.614	0.969	0.822	1.02
Average	0.038	21.6	7.69	7.67	0.752	0.931	0.510	0.932	0.586	1.01

[1] The mineralogical index of alteration calculated using Eq. 2

[2] The δEu values calculated using Eq. 1

[3] The δCe values calculated using Eq. 3

Despite the small variations in the ΣLREE/ΣHREE, the average of the ratio is almost identical for both parent rocks and bentonites, suggesting relatively equal losses/gains, if any, in the concentration of REEs during the parent-rock alteration to bentonite. As stated, the source magma composition controls the degree of enrichment in LREEs compared to HREEs, so that the larger the silica contents of the magma, the greater the enrichment in LREEs. Modabberi et al. (2019) suggested that the initial source magma composition of the studied samples was intermediate to felsic in Groups 1 and 3, and felsic in Groups 2 and 4 (Table 1), thus explaining the depletion of HREEs and Eu in most of the samples.

Because the solubility of HREE complexes is greater than that of LREEs under alkaline pH where bentonite is formed (Christidis & Huff 2009), HREEs tend to be relatively dissolved in the second phase of REE fractionation (dos Muchangos 2006), which provides an explanation for the depletion of HREEs from parent rocks to bentonites in the samples analyzed here.

Ce and Eu anomalies REEs occur exclusively in a trivalent oxidation state except for Ce and Eu, which are also found in tetravalent and divalent oxidation states, respectively. Because Ce and Eu are redox-sensitive, Ce^{4+} and Eu^{2+} may be fractionated relative to trivalent REEs, causing significant positive or negative anomalies under certain redox conditions (Elderfield 1988; Bau 1991; MacRae et al. 1992; Nath et al. 1997; Chen et al. 2015). The variation in the anomalies of Ce and Eu can be used as a proxy to study paleo-sedimentary environments and processes involved in the formation of clay minerals (Christidis 1998; Hastie et al. 2007; Özdamar et al. 2014; Liao et al. 2016; Caballero & de Cisneros 2017; Kiipli et al. 2017; Hong et al. 2019). The parent rock-normalized REE patterns of the bentonites (B/P) lead us to expect a further fractionation of REEs during the second fractionation phase (Fig. 4). To achieve a better quantitative insight into the distribution of REEs in the parent rocks, δEu and δCe values were calculated using Eqs 1 and 3, respectively (Liao et al. 2016):

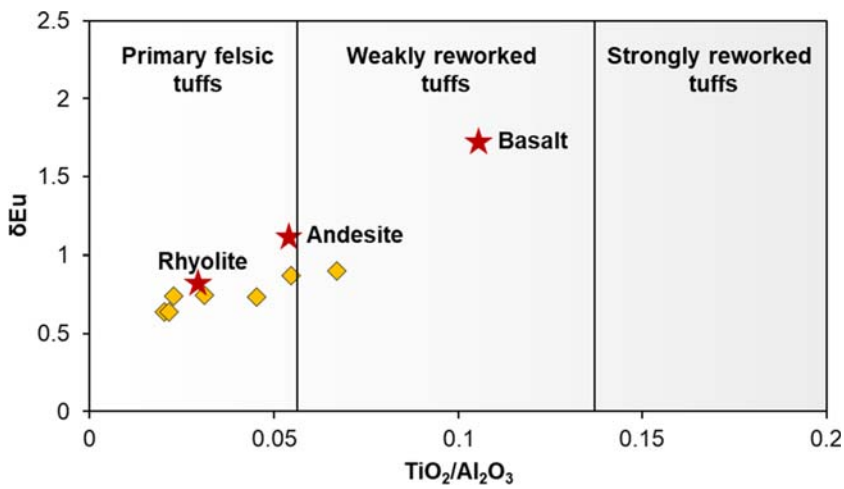

Fig. 2. Discriminant diagram of δEu vs TiO_2/Al_2O_3 of parent rocks (yellow squares) (Hong et al. 2019). Rhyolite, andesite, and basalt data (red stars) are from Laviano & Mongelli (1996).

https://doi.org/10.1007/s42860-019-00054-9 Published online by Cambridge University Press

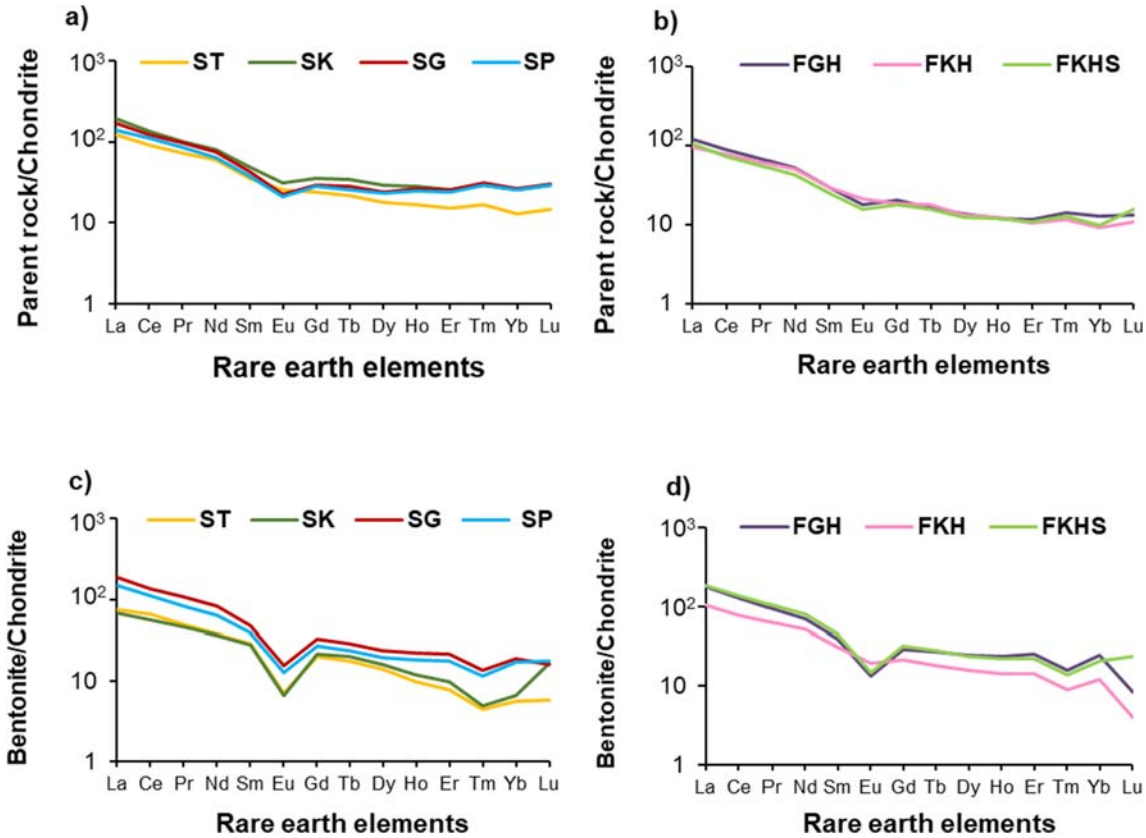

Fig. 3. Chondrite-normalized REE patterns of **a**, **b** parent rocks and **c**, **d** bentonites. Chondrite data are from McDonough & Sun (1995).

$$\delta Ce = Ce_N/(La_N \times Pr_N)^{1/2} \quad (3)$$

where the subscript N denotes chondrite-normalized.

The values of δEu and δCe for P/C, B/C, and B/P (parent rock-normalized REE patterns of bentonites) were also calculated (Table 2). The δEu values for parent rocks ranged from 0.635 to 0.902 (mean 0.752), and from 0.291 to 0.750 (mean 0.509) for bentonites, suggesting a characteristic negative anomaly for Eu in both types of samples. Regarding δCe, with the exception of ST (parent rock and bentonite), all samples showed a very flat pattern, with a very weak negative Ce negative anomaly ($1.01 > \delta Ce > 0.953$). When bentonites were normalized to parent rocks, Ce did not display any significant enrichment/depletion, showing a short range of δCe values from 0.925 to 1.17 (mean 1.01). Eu, conversely, exhibited a variable anomaly across the samples in B/P, showing a wide range of δEu values, from 0.333 to 0.831 (mean 0.590).

The δEu and δCe values of P/C were inherited chiefly from the source magma, as no advanced degree of weathering was observed in the parent rocks. In general, the δCe values were almost similar from P/C to B/C verified by the Ce values in B/P (~1.00), suggesting a relatively equal Ce loss/gain, if any, in comparison to La and Pr in the second phase of REE fractionation. ST is the only sample showing a different δCe value (0.691) in P/C. Conversely, throughout the second phase of REE fractionation, Eu was variously fractionated relative to Sm and Gd, as indicated by more pronounced negative Eu anomalies in B/C compared to P/C under increasingly oxidizing diagenetic conditions. Ce^{3+} was transformed to the relatively insoluble Ce^{4+} and, as such, it may be removed from pore waters, showing a positive anomaly through accumulation in the solid-phase sediments (Elderfield 1988; Nath et al. 1997). Chen et al. (2015) proposed that, in marine basins, the δCe value is <0.5 in oxic water (>1.5 in its solid phase sediment), ~0.6–0.9 in suboxic water (~1.1–1.4 in its solid phase sediment), and 0.9–1.0 in anoxic water (1.0–1.1 in its solid phase sediment). In other words, the larger the oxygen content in pore waters, the more Ce is removed from the water to enrich the sediment. The δCe values in B/P, hence, can be used as an indicator to evaluate the redox conditions of the local environment of the studied samples. The δCe average value was ~1.00 in all samples, suggesting a suboxic to anoxic aquatic environment for the transformation of volcanic ash to bentonite.

Eu is another highly redox-sensitive LREE, the trivalent oxidation state of which can be transformed to a more soluble divalent oxidation state under highly reducing conditions, causing the removal of Eu from the solid phase sediment (Elderfield 1988; MacRae et al. 1992; Chen et al. 2015). The depletion of Eu from parent rocks to bentonites in the second phase of REE fractionation can be ascribed to the reducing conditions where volcanic ash underwent diagenetic alteration. This confirms the hypothesis

https://doi.org/10.1007/s42860-019-00054-9 Published online by Cambridge University Press

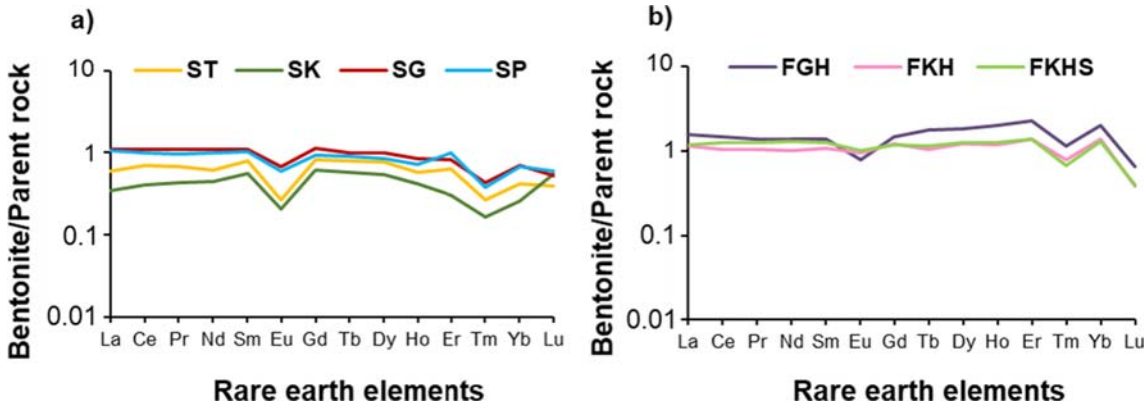

Fig. 4. Parent rock-normalized REE patterns of bentonites.

that the local environment of bentonite formation was suboxic aquatic. The depletion of Eu, however, was not the same in all the bentonite deposits, increasing from Group 1 (δEu ~0.333) to Group 4 (δEu ~0.822) as a result of local variations in the redox potential of the diagenetic environments.

Unlike Ce, which can change valence at ambient temperature, high temperature (>200°C) is another critical factor needed for the transformation of Eu^{3+} to Eu^{2+} (Nath et al. 1997). Bau (1991) calculated the Eu^{3+}/Eu^{2+} redox equilibrium for temperatures up to 600°C, suggesting that even in low redox potential, Eu exists predominantly in a divalent oxidation state with increasing temperature. Based on field observations and petrographic evidence, two types of volcanic rocks were suggested for the study area: pyroclastic flow and volcaniclastic rocks (Modabberi et al. 2019) which could provide the high temperature required for the transformation of Eu^{3+} to Eu^{2+}. Christidis & Huff (2009) reported that the alteration process is promoted at high temperatures and 300 to 850°C was suggested as a common temperature range for pyroclastic flows. Although this wide range of temperature is high enough to provide the required temperature for the reductive dissolution of Eu, it might also have a local impact on the amount of Eu^{3+} that can be transformed to Eu^{2+}.

Trace elements distribution Similar to REEs, the distribution of trace elements in bentonites is also controlled by their concentration in the parent rocks inherited from the source magma and the physiochemical conditions of the local environment, including the style of volcanic eruptions, pH, Eh, salinity, and temperature (Nesbitt 1979; Christidis 1998; Kiipli et al. 2017).

The parent rock-normalized trace element diagram was used to determine the distribution of trace elements in the bentonite samples (Fig. 5). Despite some similarities in the loss or gain of trace elements, one cannot, in general, conclude that they show the same behavior in all instances. Some relationship exists, however, among the large ion lithophile elements (LILE). Similarly, the high field strength elements (HFSE) show a significant positive correlation with each other. LILEs are characterized by large ionic radii and low valence (e.g. Ba, Rb, Sr, V, and Tl), whereas HFSEs are differentiated from other trace elements by small ionic radii and high valence states (e.g. Zr, Hf, Nb, Y) (Zielinski 1985; Summa & Verosub 1992; Fanti 2009). In the samples analyzed here, the loss/gain of trace elements was relatively equal in HFSEs; unlike LILEs, their concentrations relative to each other did not show any significant changes.

Element Mobility

Losses or gains of elements During the alteration of volcanic ash, variations in the concentration of each individual element in the residual materials are directly related to the concentration of other constituents (Nesbitt et al. 1980). Because of the dilution effect, the removal of major elements from volcanic ash and/or residual behavior of elements bring about drastic changes in the concentration of immobile materials (Kiipli et al. 2017). Residual behavior occurs when elements are essentially immobile so that their concentrations increase through the depletion of mobile elements from the environment (Christidis 1998; Kiipli et al. 2017; Hong et al. 2019). Study of the behavior of immobile elements during the devitrification of volcanic ash is imperative, as increases or decreases in their concentrations show the degree to which other elements are lost or gained (Nesbitt et al. 1980; Christidis 1998; Kiipli et al. 2017).

Instead of using the absolute concentration of elements in analyzing their mobility, Nesbitt (1979) suggested use of the element's ratio to an immobile element, as this ratio is not influenced by the dilution effect. Al has commonly been considered an immobile element during the chemical weathering, transport, diagenesis, and metamorphism of volcanic ash (Nesbitt 1979; Slack & Stevens 1994; Laviano & Mongelli 1996; Christidis 1998; Göncüoglu et al. 2016; Kiipli et al. 2017; Hong et al. 2019) which makes it an appropriate choice for studying the percentage changes in the concentration of elements during the alteration process.

The percentage changes relative to parent rocks were calculated following Nesbitt et al. (1980):

$$\%\text{change} = \left[\left(R_s - R_p\right)/R_p\right] \times 100 \quad (4)$$

where R_s and R_p are the concentrations of an element in a

https://doi.org/10.1007/s42860-019-00054-9 Published online by Cambridge University Press

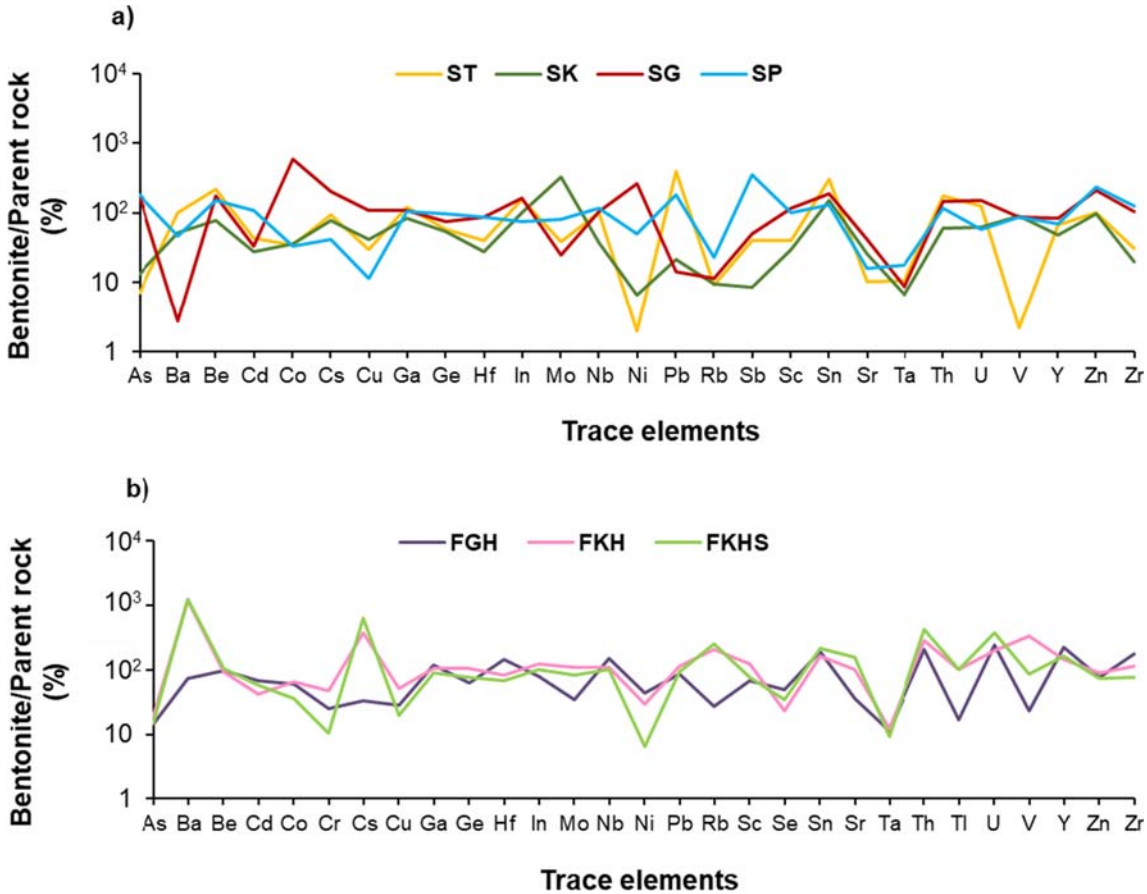

Fig. 5. Parent rocks-normalized trace elements patterns of bentonites. Only the patterns of those elements are given that showed a concentration above the detection limit of the method.

bentonite and its parent rock, respectively, each of which is normalized to the corresponding Al %. In addition, the absolute concentrations of Al in bentonites and parent rocks were used to measure the percentage change of Al itself to determine whether other elements were lost or gained (Nesbitt 1979):

$$\%\text{change} = \left[\left(Al_s – Al_p\right)/Al_p\right] \times 100 \quad (5)$$

where Al_s is the concentration of Al in a bentonite and Al_p is the concentration of Al in the corresponding parent rock.

The percentage changes in elements during alteration of volcanic ash to bentonite (Table 3) revealed that the average amount of Al lost was small (~12.5%) among all the deposits and this agrees well with the literature which has reported Al as an immobile to poorly mobile element (Nesbitt 1979; Slack & Stevens 1994; Laviano & Mongelli 1996; Christidis 1998; Göncüoglu et al. 2016; Kiipli et al. 2017; Hong et al. 2019). Although the variation of Al concentration was not significant in most of the samples, the loss of Al was found to be large in a few samples such as SK (–34.1%). The changes observed in Al concentration may be the result of the dilution effect caused by losses or gains of other major elements such as Si, which is the predominant element in both parent rocks and bentonites. The most negative percentage change in Al concentration was observed in SK, where Si showed the most positive percentage change (59.42%). When the percentage changes of Al and Si were plotted against each other (Fig. 6), they exhibited an inversely proportional trend, with $R^2 > 90$, suggesting a significant inverse correlation.

Ithough the concentration of Al is more or less controlled by the variation in the Si concentration, it may not be enough to explain the –34.1% decrease in the Al concentration of the SK sample. The initial volcanic ash from which bentonites formed was deposited in an aqueous environment which increased the water content of the samples during the hydrolysis reaction that converts the volcanic ash to bentonite. The loss on ignition (LOI) increased considerably in all the samples during alteration, but this value was significantly larger in the SK sample (~1909%) (Table 3). Increasing the water content of the samples caused the residual elements such as Al to be diluted, providing another explanation for the decrease in the Al content of the SK sample. The variation in the LOI content of the samples showed that the physiochemical condition during the formation of bentonites was locally different.

https://doi.org/10.1007/s42860-019-00054-9 Published online by Cambridge University Press

Table 3 Percentage change of elements during the alteration of volcanic ash.

	Group 1		Group 2		Group 3		Group 4
	ST %	SK %	SG %	SP %	FGH %	FKH %	FKHS %
Si	21.9	59.4	–4.75	17.8	–9.89	8.36	–16.1
Al	–25.4	–34.1	0.435	–16.2	3.06	–12.6	10.6
Fe	–67.1	–39.6	266	179	–50.7	–43.8	167
Mg	687	701	2245	462	153	–20.1	1109
Ca	–75.5	–78.5	–4.85	–53.0	–76.6	209.9	14.9
Na	81.3	11.6	–26.7	–32.3	165	–14.6	38.9
K	–94.4	–97.2	–96.7	–84.8	–80.9	–40.2	–91.1
Ti	–98.3	–96.1	–14.8	–23.6	–48.9	–7.21	8.30
P	–82.1	–78.3	–50.3	–20.4	–3.03	–17.4	–38.0
Mn	–55.3	–1.30	98.9	–40.3	–78.7	–42.8	80.5
LOI	945	1909	405	79.7	132	178	205
As	–90.2	–79.6	75.1	120.9	–86.3	–77.9	–54.0
Ba	37.5	–20.9	–97.2	–44.5	–28.0	1261	–4.48
Be	196	19.9	76.3	83.0	–7.43	7.64	80.5
Cd	–41.4	–57.8	–66.8	32.6	–35.4	–51.0	ND
Co	–53.8	–44.1	486	–60.2	–42.5	–24.1	70.0
Cr	–33.0	–24.1	–33.7	ND	–75.8	–46.5	–39.8
Cs	28.0	17.6	107	–49.3	–68.0	331	673
Cu	–56.5	–32.5	9.47	–86.3	–72.5	–41.7	–88.5
Ga	65.9	27.7	7.52	26.1	12.8	18.7	13.0
Ge	–22.5	–16.1	–25.2	17.7	–38.8	21.3	–30.6
Hf	–45.2	–58.0	–12.3	3.91	41.4	–6.67	0.282
Hg	ND	ND	ND	ND	–3.03	ND	–54.9
In	114.4	51.8	65.8	–10.5	–22.4	43.0	80.5
Li	ND	ND	ND	ND	ND	ND	ND
Mo	–48.5	–87.3	–75.1	–4.50	–66.4	24.8	–37.5
Nb	34.8	–42.7	2.97	40.4	44.6	26.5	15.8
Ni	–73.2	1.23	165.2	–40.3	–56.9	–66.3	1.54
Pb	435	–67.2	–85.6	114.7	–16.0	30.0	138
Rb	–87.4	–85.4	–88.4	–71.9	–73.4	132	–74.0
Re	ND	ND	ND	ND	ND	ND	ND
Sb	–46.4	–86.8	–50.3	318	–67.7	ND	35.4
Sc	–46.4	–54.4	16.0	19.4	–35.4	39.8	216
Se	–24.1	–46.9	72.4	ND	–51.5	–73.5	–61.9
Sn	313	131	91.3	59.2	84.7	84.7	57.9
Sr	–86.1	–60.9	–59.0	–80.7	–64.6	16.4	–73.2
Ta	–85.7	–89.8	–91.4	–78.9	–89.2	–86.0	–90.9
Te	ND	ND	ND	ND	ND	ND	ND
Th	135	–9.0	45.6	39.9	97.8	223	15.1
Tl	ND	–87.3	ND	ND	–83.8	14.4	–54.9
U	70.2	–4.4	51.9	–29.8	133	129	117
V	–97.1	28.6	–13.0	4.5	–77.4	275	76.4
Y	–9.7	–24.8	–15.1	–15.4	115	64.8	26.8
Zn	36.0	47.0	111	179	–27.4	2.2	2.8
Zr	–58.8	–68.9	4.0	48.7	67.7	28.7	31.6
La	–19.2	–47.7	9.18	26.7	48.9	28.8	7.72
Ce	–4.98	–37.9	8.28	19.0	40.4	18.0	14.4
Pr	–9.76	–33.2	9.06	16.4	33.8	17.2	13.7
Nd	–16.6	–32.0	8.89	20.2	34.1	16.4	16.9
Sm	8.36	–14.3	9.6	22.8	34.4	20.7	14.4
Eu	–63.7	–68.1	–32.7	–29.4	–24.6	7.52	–8.72
Gd	9.29	–7.74	13.0	10.8	42.7	38.9	7.75
Tb	5.51	–13.2	0.421	7.95	70.1	19.8	3.15
Dy	3.13	–17.6	–1.88	1.16	77.2	37.6	14.5
Ho	–22.2	–35.9	–15.2	–14.0	95.5	34.8	11.4
Er	–30.5	–42.8	–17.5	–13.5	119	58.9	22.3
Tm	–64.1	–74.7	–57.4	–54.2	10.8	–10.1	–38.9
Yb	–43.5	–60.6	–30.1	–20.0	92.5	57.3	17.8
Lu	–47.9	–15.6	–47.6	–28.0	–36.4	–56.0	–64.4

The smallest variation in Al concentration was observed in the SG sample (~0.4%). To evaluate the mobility of elements, several samples from this deposit (Chah-Golestan) were used to decrease the impact of local geochemical and lithological conditions. This will be discussed further below.

As stated, Al has been considered consistently as an immobile element and, thus, ∽–35% change, which is the most negative percentage change in Al concentration, can loosely be regarded as a plausible threshold to identify potential immobile elements, as the percentage changes in the Al concentration mostly result from the dilution effect. Similarly, elements showing a positive percentage (residual enrichment) were also proposed by Christidis (1998) to be considered immobile. For the purpose of the present study, those elements displaying positive percentage changes, or negative changes smaller than –35% in more than half of the deposits (4 of 7), were hypothesized as potential immobile elements, including Si, Al, Na, Mg, Be, Ga, In, U, Y, Zn, Pr, Nd, Sm, Gd, Tb, Dy, Ti, Ba, Cs, Ge, Nb, Pb, Sc, Sn, Th, V, Zr, La, Ce, Eu, Er, Yb, Hf, and Ho. At the current stage of the study, in no case has the immobility of any of these elements been proved. This method was used solely to achieve an understanding of the potential immobile elements, and further analysis is needed to evaluate the mobility of the elements.

Statistical analysis The results of bivariate correlation analyses (Tables 4 and 5), calculated using the percentage changes provided in Table 3, showed that besides the expected negative correlation with Al ($r > -0.953$), Si also displayed an inverse correlation with LREEs. A positive correlation ($r > 0.900$) existed between HFSEs and REEs. Both LREEs and HREEs have positive correlations with other elements of their group ($r > 0.950$), but the r values fall to <0.850 when LREEs are compared with HREEs. Eu exhibited a less significant correlation with other REEs ($R < 0.800$), while no significant correlation was found between Lu and HREEs.

https://doi.org/10.1007/s42860-019-00054-9 Published online by Cambridge University Press

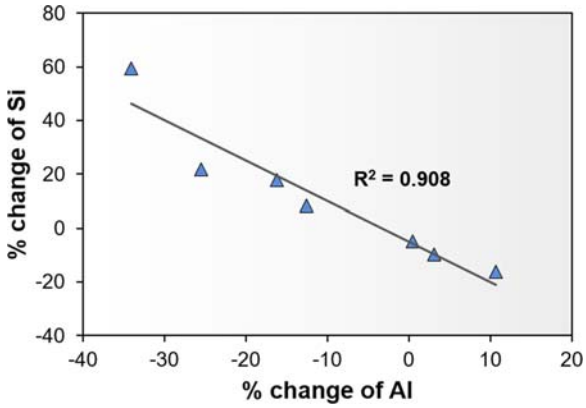

Fig. 6. The inverse correlation between the percentage changes of Al

Some unexpected elements (e.g. Si and Na) appeared among the potential immobile elements in the previous section, as they have been reported to be actively mobile (Caballero et al. 1992; Christidis et al. 1995; Christidis & Huff 2009). The binary diagram was plotted using Chah-Golestan (SG) bentonite and parent rock samples to evaluate the mobility of each of the elements provided in the list of potential immobile elements (Fig. 7a and b). The largest deposit in the studied area was SG, where various layers of bentonite are exposed at the surface. These exposed layers provided numerous samples from this deposit (instead of using samples from different deposits) which were used in the binary diagrams to decrease the impact of local geochemical and lithological conditions, supposedly affecting the mobility of element. Overall, seven bentonites and two volcanic rocks from Chah-Golestan were used in the binary diagrams (see Table B in the SI). The SG2 sample is the parent rock of the samples SG-D, SG-E, SG-F, and SG-G where the gradual transition of SG2 to SG-G could be observed clearly (Fig. 1). The samples SG-A, SG-B, and SG-C (bentonite) and SG3 (volcanic rock) were also taken from other horizons of the Chah-Golestan deposit to increase the diversity of the samples in the binary diagrams and ensure that samples were taken from the different sections of the deposit.

If two different chemical elements of several bentonites are immobile during the alteration of volcanic ash to bentonite, they should show a strong correlation, with the least squares line (R^2) passing through the origin of the binary diagram. Two such elements should be considered immobile, as two elements with distinctly different chemical properties are unlikely to be of equal solubility and mobility (Christidis 1998; Kiipli et al. 2017).

Based on the correlation of each element with the least squares line, i.e. R^2 values (Fig. 8), the mobility of elements was loosely classified into three groups: immobile, poorly mobile, and mobile. Note that the following is merely a qualitative classification because choosing a definitive boundary delineating each group of elements may not be applicable at this stage of the study. The elements with R^2 values > 0.800 (80% accuracy) were thus proposed to be considered immobile, as Kiipli et al. (2017) also found the R^2 values up to 0.73 to be relatively low. For the purpose of the present study, elements with R^2 values between of < 0.500 and 0.800 were also considered to be poorly mobile and those with values < 0.500 were considered to be mobile.

The highest R^2 values (0.800–1.00) were observed in Ti, Gd, Ga, Pr, Tb, Nd, Sm, Ce, and Nb, all of which were included in the list of potential immobile elements. Along with Al, they were probably immobile during bentonite formation. Regression lines pointing to the origin of the chart for Sc, Hf, U, Dy, In, Zr, La, and Eu show less correlation, with R^2 values between 0.500 and 0.800. These elements were also included in the list of potential immobile elements but, because of the lower R^2 values, they cannot be verified as being immobile, so they are classified in the poor-mobility group. In addition, the elements (Si, Na, Mg, Be, Y, Zn, Ba, Cs, Ge, Pb, Th, V, Er, and Yb) with $R^2 < 0.500$ were certainly mobile during bentonite formation; therefore, they are listed in the mobile elements group. Most of the elements classified here as immobile or of low mobility agree quite well with those reported in the literature on mobility of elements throughout volcanic ash transformation (Nesbitt 1979; Nesbitt et al. 1980; Zielinski 1985; Christidis 1998; dos Muchangos 2006; Özdamar et al. 2014; Kacmaz 2016; Liao et al. 2016; Kiipli et al. 2017; Hong et al. 2019).

Major element mobility The results demonstrate that even elements displaying strong residual enrichment such as Si (up to ~60%) and Na (up to ~80%) may not be immobile, as shown in the binary diagram analysis (Fig. 7b). The release of Si from volcanic ash to the aqueous environment is a critical factor in the formation of bentonite (Christidis & Huff 2009). Despite the alteration of volcanic ash to bentonite, the Si fraction that was apparently washed off the parent rocks was not leached entirely from the environment, even exhibiting strong residual enrichment in some of the deposits. The mineralogy of bentonite samples in eastern Iran showed that the bentonite samples are not composed entirely of smectite minerals (Na-montmorillonite), and they include up to 39% of opaline silica (i.e. opal-CT and opal-C) as a secondary phase (Table 1). Given this, a fraction of Si was indeed depleted from the volcanic ash but precipitated and subsequently crystallized to opaline silica in situ. Modabberi et al. (2019) reported that in the eastern Iranian bentonite zone, the water/rock ratio, which is one of the factors controlling the availability of Si in the system during alteration, was low. At higher water/rock ratios in an open system, the free Si released from the volcanic ash may not precipitate to any great extent, accumulating instead in the fluid phase and leaching out of the environment (Christidis & Huff 2009). Overall, Si was depleted from the volcanic ash, showing

https://doi.org/10.1007/s42860-019-00054-9 Published online by Cambridge University Press

https://doi.org/10.1007/s42860-019-00054-9 Published online by Cambridge University Press

Table 4 The bivariate correlation analysis of Si with Al, HFSEs, and REEs[1]0.

	Si	Al	Hf	Nb	Rb	Y	Zr	La	Ce	Pr	Nd	Sm	Eu	Gd	Tb	Dy	Ho	Er	Tm	Yb	Lu
Si	1																				
Al	–0.953**	1																			
Hf	–0.780*	0.771*	1																		
Nb	–0.622	0.405	0.678	1																	
Rb	–0.081	–0.014	0.123	0.178	1																
Y	–0.555	0.524	0.763*	0.511	0.420	1															
Zr	–0.749	0.745	0.963**	0.654	0.248	0.659	1														
La	–0.761*	0.678	0.947**	0.782*	0.343	0.729	0.951**	1													
Ce	–0.844*	0.747	0.949**	0.845*	0.235	0.731	0.925**	0.978**	1												
Pr	–0.855*	0.781*	0.958**	0.790*	0.269	0.721	0.952**	0.985**	0.994**	1											
Nd	–0.833*	0.795*	0.971**	0.724	0.246	0.689	0.985**	0.976**	0.971**	0.989**	1										
Sm	–0.752	0.627	0.920**	0.901**	0.261	0.736	0.894**	0.967**	0.985**	0.965**	0.935**	1									
Eu	–0.704	0.685	0.676	0.447	0.674	0.598	0.791*	0.761*	0.720	0.774*	0.794*	0.663	1								
Gd	–0.579	0.456	0.752	0.668	0.582	0.893**	0.694	0.849*	0.817*	0.808*	0.750	0.833*	0.667	1							
Tb	–0.516	0.451	0.818*	0.645	0.150	0.909**	0.670	0.773*	0.785*	0.751	0.708	0.816*	0.373	0.859*	1						
Dy	–0.590	0.528	0.814*	0.622	0.340	0.983**	0.696	0.790*	0.801*	0.780*	0.737	0.815*	0.550	0.919**	0.964**	1					
Ho	–0.609	0.585	0.845*	0.558	0.312	0.986**	0.733	0.793*	0.797*	0.788*	0.762*	0.796*	0.580	0.891**	0.951**	0.992**	1				
Er	–0.614	0.592	0.842*	0.546	0.393	0.990**	0.753	0.805*	0.799*	0.797*	0.776*	0.795*	0.649	0.903**	0.921**	0.984**	0.995**	1			
Tm	–0.617	0.573	0.829*	0.579	0.490	0.983**	0.762*	0.831*	0.814*	0.814*	0.788*	0.814*	0.705	0.940**	0.897**	0.975**	0.979**	0.992**	1		
Yb	–0.652	0.619	0.843*	0.576	0.486	0.976**	0.789*	0.834*	0.824*	0.828*	0.810*	0.817*	0.747	0.913**	0.869*	0.961**	0.971**	0.989**	0.995**	1	
Lu	0.746	–0.641	–0.254	–0.403	–0.365	–0.295	–0.289	–0.341	–0.440	–0.449	–0.395	–0.362	–0.640	–0.346	–0.074	–0.263	–0.246	–0.286	–0.332	–0.376	1

[1] The bivariate correlation of elements was calculated using the percentage changes provided in Tables 4 and 5.

**Correlation is significant at the 0.01 level

*Correlation is significant at the 0.05 level

Table 5 The bivariate correlation analysis of Si with Al and LILEs[1]0.

	Si	Al	Ca	K	Ba	Rb	Sr	Th	Tl	V
Si	1									
Al	–0.953**	1								
Ca	–0.268	0.205	1							
K	–0.177	0.069	0.866*	1						
Ba	–0.026	–0.082	0.918**	0.950**	1					
Rb	–0.081	–0.014	0.933**	0.972**	0.993**	1				
Sr	–0.044	0.012	0.908**	0.893**	0.936**	0.947**	1			
Th	–0.196	–0.039	0.656	0.812*	0.813*	0.786*	0.672	1		
Tl	–0.236	0.075	1.000**	0.914	0.955*	0.959*	0.906	0.828	1	
V	–0.032	0.051	0.928**	0.801*	0.865*	0.885**	0.874*	0.431	0.946	1

[1] The bivariate correlation of elements was calculated using the percentage changes provided in Tables 4 and 5.

**Correlation is significant at the 0.01 level

*Correlation is significant at the 0.05 level

strong mobility, but fluid flow volume was not sufficient to leach it from the environment, i.e. any residual enrichment does not equal immobility. In all instances, the SiO_2/Al_2O_3 ratio is significant (up to 7), and thus, the variation in the concentration of Si has a considerable impact on that of the other elements in general and immobile elements in particular.

The behavior of alkalies during volcanic-ash transformation governs the formation of either smectites or zeolites; if the alkalies are not removed from the system, the $(Na^+ + K^+)/H^+$ ratio increases and, instead of smectites, zeolites are formed (Christidis et al. 1995; Yildiz & Kuscu 2004). The absence of zeolites in the samples studied suggests that alkalies were leached out of the environment to some extent. The changes in K percentage showed substantial depletion in all deposits (up to 97%), while Na seems to be less mobile across the deposits and acts as a counter cation in the structure of Na-montmorillonite, which is the main mineralogical phase in the samples studied (Table 3).

The large $(Mg^{2+})/(H^+)$ ratio and leaching of alkali elements from the aqueous environment promotes the destabilization of the plagioclase structure and provides a suitable pH (~8) for the formation of bentonite instead of zeolite (Christidis 1998; Christidis & Huff 2009; Modabberi et al. 2019). Christidis & Huff (2009) suggested that in the transformation of acidic parent rocks with a small Mg content, the required Mg is supplied by the fluid phase. The concentration of Mg has increased significantly from the parent rocks to bentonites in all the samples studied with the exception of FKH (Table 3), suggesting the addition of Mg to the bentonite samples from the aqueous environment. Because the FKH sample is not acidic in composition, it did not need to take up Mg from the aqueous environment as its parent rock already had the largest concentration of Mg (2.60%) across the samples.

Trace and rare earth element mobility All the LILEs were listed in the mobile group of the classification provided. The alkaline trace elements such as Rb and alkaline earth metals (e.g. Ba and Sr), known mostly as LILE, are highly mobile in aqueous environments (Zielinski 1985; Khan 1990; Hong et al. 2019). They display pronounced positive correlations ($r > 0.950$) with K (i.e. alkaline metal) and Ca (i.e. alkaline earth metal) which are geochemically similar major elements (Tables 4 and 5). Biotite, feldspar, and K-feldspar host Ba and Rb in volcanic ash, rapidly releasing these mobile elements during alteration (Renock et al. 2016). Although LILEs show a positive correlation with K, their contents are not controlled significantly by K-bearing minerals but by sorption on the surface of bentonite (Nesbitt et al. 1980; Hodson 2002).

HFSEs are commonly considered less soluble and relatively immobile elements, preserving the characteristics of the source materials (Merriman & Roberts 1990; Huff et al. 1993; Pellenard et al. 2003; Calarge et al. 2006). Zr, Hf, and Nb are listed in the immobile to poorly mobile groups, while some other HFSEs, such as Y, Ta, and Th, showed some degree of mobility (Fig. 8). During the diagenetic alteration of volcanic ash, authigenic clay minerals are formed in situ, and, therefore, their immobile contents may not be fractionated and may be mostly inherited from the source magma composition. The physiochemical conditions (pH, Eh, salinity) of the local environment are also important factors controlling the mobility of trace elements and possibly causing some redistribution of immobile elements (Hong et al. 2019). For instance, while Zr and Y are known as immobile elements in the literature (Nesbitt 1979; Christidis 1998; Kiipli et al. 2017), they were found to be poorly mobile and mobile, respectively, in these samples (Fig. 8). Zr and Y are incorporated

https://doi.org/10.1007/s42860-019-00054-9 Published online by Cambridge University Press

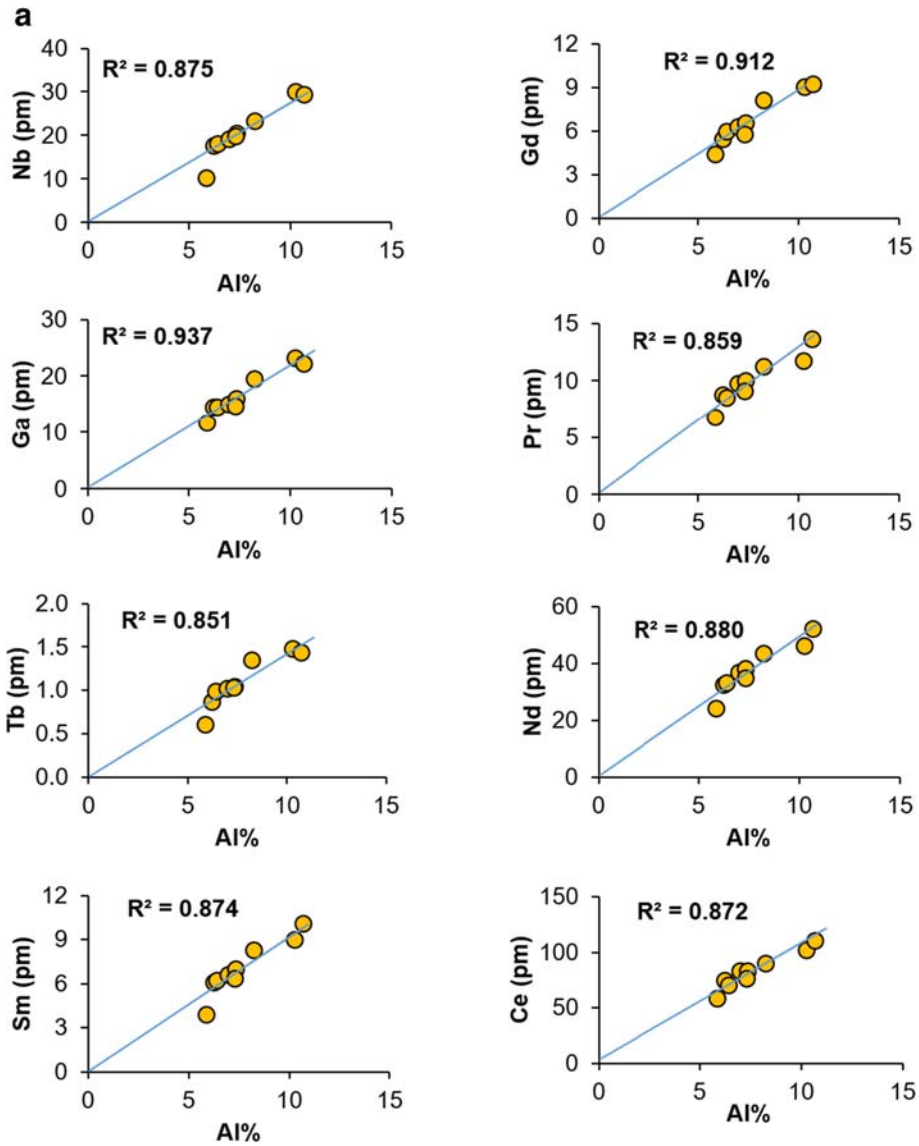

Fig. 7. **a** Representative binary diagrams of Al vs potential immobile elements with R^2 values >0.800 for the bentonites and parent rocks of Chah-Golestan deposit. **b** The representative binary diagrams of Al vs potential immobile elements with R^2 values (a, b, c, d) between 0.500 and 0.800, and (e, f, g, h) < 0.500 for the bentonites and parent rocks of the Chah-Golestan deposit. The negative R^2 value for the Al vs Si line is because the intercept was set at zero, forcing the line to pass through the origin.

into the structure of early-crystallized heavy minerals such as zircon, garnet, and monazite. These minerals are very sensitive to physical sorting in aqueous environments, and hence, susceptible to being leached as colloidal phases thereby removing Zr and Y from the open system (Summa & Verosub 1992; Wray 1995; Hong et al. 2019).

Because of similar geochemical characteristics, REEs are also classified as HFSEs (Zielinski 1985; Summa & Verosub 1992; Fanti 2009; He et al. 2014), showing a strong positive correlation with their equivalent trace elements such as Zr and Hf (Tables 4 and 5). All of the LREEs and Gd, Tb, and Dy from the HREEs were found to be either immobile or poorly mobile (Fig. 8). HREEs show a degree of mobility indicating that the heavier the element, the more mobile it is during volcanic ash conversion. LREEs have been proposed to be less soluble and retain their concentration in an alkaline solution, while HREEs favor making complexes in the aqueous phase, causing their removal from the solid phase-sediments (Summa & Verosub 1992; dos Muchangos 2006). The various dissolution behaviors shown by REEs may explain the greater mobility of some of the heavier HREEs such as Er compared to lighter HREEs such as Gd and Tb. Summa & Verosub (1992) stated that the degree to which HREEs

https://doi.org/10.1007/s42860-019-00054-9 Published online by Cambridge University Press

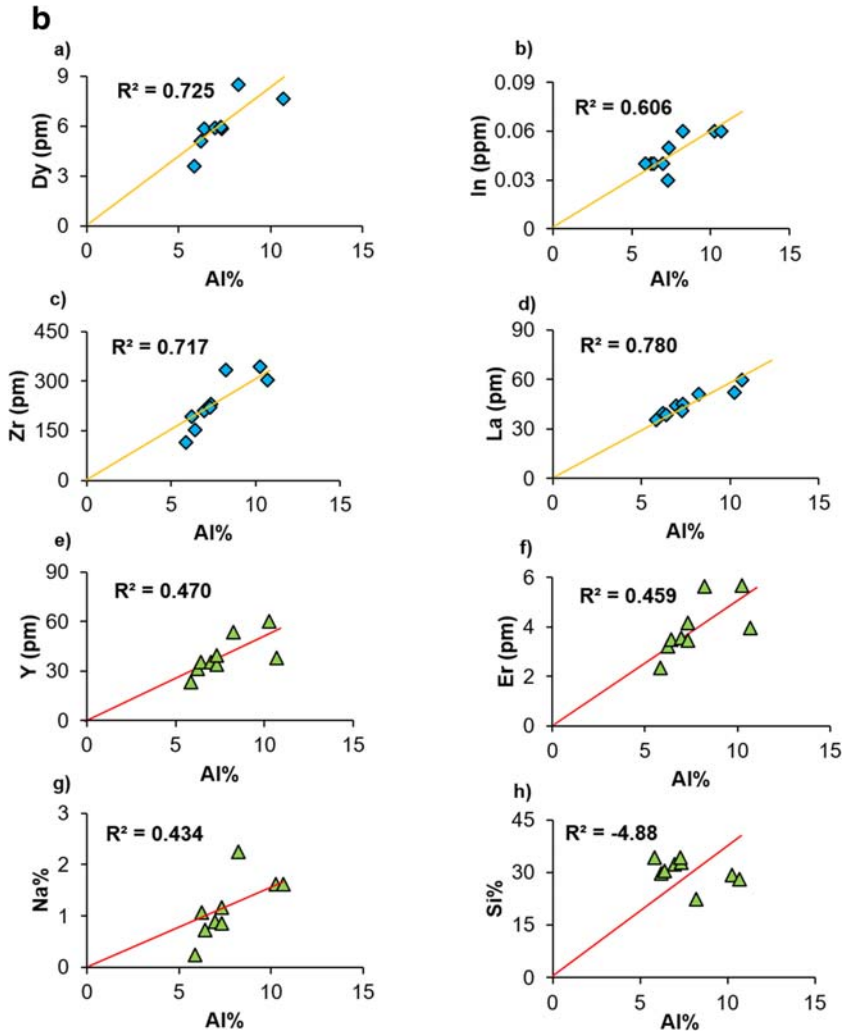

Fig. 7 continued.

accumulate in the fluid phase is controlled by the water/rock ratio such that their mobility increases in dense solutions (i.e. low water/rock ratio). Modabberi et al. (2019) proposed a shallow aqueous environment with a low water/rock ratio, such as a lagoon, as the aqueous environment in which the eastern Iranian bentonites were formed, which explains the greater mobility of HREEs.

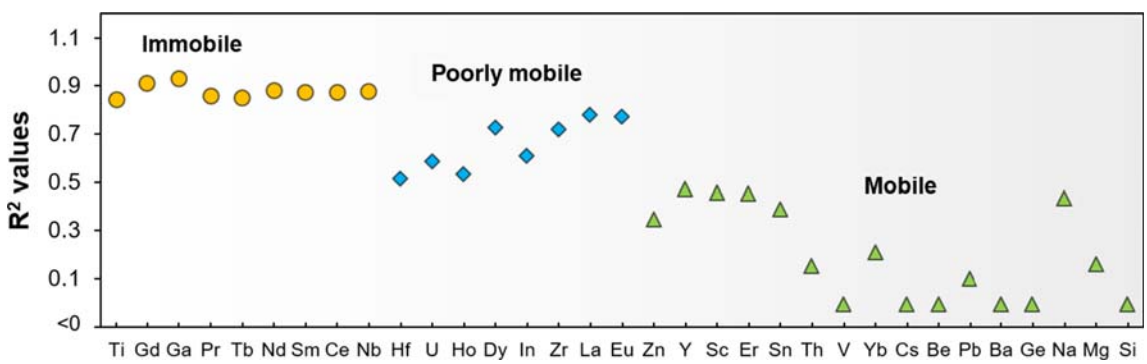

Fig. 8. Qualitative estimate of the mobility of elements during the alteration of volcanic ash to bentonite for the eastern Iranian bentonite deposits. The R^2 values were obtained from the binary diagrams of Al vs potential immobile elements. For the binary diagram with $-R^2$, the real values are not shown here, and all of them are represented as <0.

https://doi.org/10.1007/s42860-019-00054-9 Published online by Cambridge University Press

CONCLUSIONS

The present study examined the distribution and mobility of trace elements and REEs during the alteration of volcanic ash to bentonite in the eastern Iranian bentonite zone. The degree of weathering in the parent rocks was evaluated, suggesting that the parent rocks were not influenced significantly by an advanced degree of depositional reworking and, as such, are an accurate representation of the volcanic ash from which the bentonites were formed. The ΣLREE/ΣHREE ratios and the chondrite-normalized REE patterns of both parent rocks and bentonites showed that LREEs were enriched in comparison to HREEs, owing to their concentration in the source magma and the physiochemical conditions of the aqueous environment. The variation in the δCe and δEu values suggests that the diagenetic alteration of volcanic ash probably occurred in a suboxic aquatic environment. In general, trace elements did not display any identical pattern of enrichment/depletion, but both LILEs and HFSEs showed some similar behavior between the elements of their respective groups in the parent rock-normalized trace element diagram.

The percentage changes in the concentration of immobile elements seem to be influenced primarily by the behavior of Si, as it shows a significant negative correlation with Al and LREEs. Furthermore, in the bivariate correlation analysis, LILEs, HFSEs, HREEs, and LREEs displayed a positive correlation between the elements of their respective groups. Based on the results obtained from the binary diagram of potential immobile elements vs Al, a qualitative classification was proposed for different mobility behaviors, consisting of an immobile group, attributed to R^2 values of >0.800, a poorly mobile group, with R^2 values between 0.500 and 0.800, and a mobile group, corresponding to R^2 values <0.500. Accordingly, Ti, Gd, Ga, Pr, Tb, Nd, Sm, Ce, and Nb are considered immobile, and U, Dy, In, Sc, Hf, Zr, La, and Eu are considered to be poorly mobile during the alteration of volcanic ash to bentonite.

Overall, a systematic study of the behavior of trace elements and REEs during the devitrification of volcanic ash has helped to determine the magmatism and tectonic setting of source volcanism, and to correlate the ash layers of different areas. This study showed that the physiochemical conditions of the local environment control to a significant extent the behavior of elements, and, therefore, the diagenetic histories of the area studied should be taken into careful consideration prior to use of trace elements and REEs for study of the source magma.

ACKNOWLEDGMENTS

This research was partly funded by the Iran National Science Foundation (contract no. 90004849), Spanish Group CTS-946 (Junta de Andalucia), and MINECO project CGL2016-80833-R. The authors acknowledge the School of Geology of the University of Tehran for sample preparation and some geochemical tests. The authors express their gratitude to Shaghayegh V. Navabpour for assisting with the statistical analyses. They also sincerely thank the reviewers for their careful reading of the manuscript and their many insightful comments and suggestions which certainly helped to improve the manuscript.

Compliance with ethical standards

Conflict of Interest

The authors declare that they have no conflict of interest.

Ethical approval

This article does not contain any studies with human participants or animals performed by any of the authors.

Informed consent

Informed consent was obtained from all individual participants included in the study.

REFERENCES

Arslan, M., Abdioğlu, E., & Kadir, S. N. (2010). Mineralogy, geochemistry, and origin of bentonite in Upper Cretaceous pyroclastic units of the Tirebolu area, Giresun, northeast Turkey. *Clays and Clay Minerals, 58*, 120–141.

Batchelor, R. A. (2014). Metabentonites from the Sandbian stage, Upper Ordovician, in Scotland–a geochemical comparison with their equivalents in Baltoscandia. *Scottish Journal of Geology, 50*, 159–163.

Batchelor, R. A., & Evans, J. (2000). Use of strontium isotope ratios and rare earth elements in apatite microphenocrysts for characterization and correlation of Silurian metabentonites: A Scandinavian case study. *Norsk Geologisk Tidsskrift, 80*, 3–8.

Bau, M. (1991). Rare-earth element mobility during hydrothermal and metamorphic fluid-rock interaction and the significance of the oxidation state of europium. *Chemical Geology, 93*, 219–230.

Berberian, M., & King, G. (1981). Towards a paleogeography and tectonic evolution of Iran. *Canadian Journal of Earth Sciences, 18*, 210–265.

Brantley, S. L. (2008). Kinetics of mineral dissolution. In S. L. Brantley, J. D. Kubicki, & A. F. White (Eds.), *Kinetics of Water-rock Interaction* (pp. 151–210). New York: Springer New York.

Burger, K., Zhou, Y., & Ren, Y. (2002). Petrography and geochemistry of tonsteins from the 4th member of the Upper Triassic Xujiahe formation in southern Sichuan province, China. *International Journal of Coal Geology, 49*, 1–17.

Caballero, E., & de Cisneros, C. J. (2017). Partitioning of minor, trace elements and rare earth elements in bentonite affecting by thermal alteration. *Applied Clay Science, 147*, 143–152.

Caballero, E., Reyes, E., Delgado, A., Huertas, F., & Linares, J. (1992). The formation of bentonite: Mass balance effects. *Applied Clay Science, 6*, 265–276.

Calarge, L. M., Meunier, A., Lanson, B., & Formoso, M. L. (2006). Chemical signature of two Permian volcanic ash deposits within a bentonite bed from Melo, Uruguay. *Anais da Academia Brasileira de Ciências, 78*, 525–541.

Chen, J., Algeo, T. J., Zhao, L., Chen, Z.-Q., Cao, L., Zhang, L., & Li, Y. (2015). Diagenetic uptake of rare earth elements by bioapatite, with an example from Lower Triassic conodonts of south China. *Earth-Science Reviews, 149*, 181–202.

Chorover, J., & Brusseau, M. L. (2008). Kinetics of sorption—desorption. In S. L. Brantley, J. D. Kubicki, & A. F. White (Eds.), *Kinetics of Water-rock Interaction* (pp. 109–149). New York: Springer New York.

Christidis, G. E. (1998). Comparative study of the mobility of major and trace elements during alteration of an andesite and a rhyolite to

https://doi.org/10.1007/s42860-019-00054-9 Published online by Cambridge University Press

bentonite, in the islands of Milos and Kimolos, Aegean, Greece. *Clays and Clay Minerals, 46*, 379–399.

Christidis, G. (2001). Geochemical correlation of bentonites from Milos Island, Aegean, Greece. *Clay Minerals, 36*, 295–306.

Christidis, G. E., & Huff, W. D. (2009). Geological aspects and genesis of bentonites. *Elements, 5*, 93–98.

Christidis, G. E., Scott, P. W., & Marcopoulos, T. (1995). Origin of the bentonite deposits of eastern Milos, Aegean, Greece; geological, mineralogical and geochemical evidence. *Clays and Clay Minerals, 43*, 63–77.

Dai, S., Wang, X., Zhou, Y., Hower, J. C., Li, D., Chen, W., Zhu, X., & Zou, J. (2011). Chemical and mineralogical compositions of silicic, mafic, and alkali tonsteins in the late Permian coals from the Songzao coalfield, Chongqing, southwest China. *Chemical Geology, 282*, 29–44.

Dai, S., Ward, C. R., Graham, I. T., French, D., Hower, J. C., Zhao, L., & Wang, X. (2017). Altered volcanic ashes in coal and coal-bearing sequences: A review of their nature and significance. *Earth-Science Reviews, 175*, 44–74.

dos Muchangos, A. C. (2006). The mobility of rare-earth and other elements in the process of alteration of rhyolitic rocks to bentonite (Lebombo volcanic mountainous chain, Mozambique). *Journal of Geochemical Exploration, 88*, 300–303.

Elderfield, H. (1988). The oceanic chemistry of the rare-earth elements. *Philosophical Transactions of the Royal Society of London, A, 325*, 105–126.

Elliott, W. C., Gardner, D. J., Malla, P., & Riley, E. (2018). A new look at the occurrences of the rare-earth elements in the Georgia kaolins. *Clays and Clay Minerals, 66*, 245–260.

Fanti, F. (2009). Bentonite chemical features as proxy of late Cretaceous provenance changes: A case study from the western interior basin of Canada. *Sedimentary Geology, 217*, 112–127.

Foreman, B., Rogers, R., Deino, A., Wirth, K., & Thole, J. (2008). Geochemical characterization of bentonite beds in the Two Medicine formation (Campanian, Montana), including a new $^{40}Ar/^{39}Ar$ age. *Cretaceous Research, 29*, 373–385.

Göncüoglu, M., Günal-Türkmenoglu, A., Bozkaya, Ö., Ünlüce-Yücel, Ö., Okuyucu, C., & Yilmaz, İ. (2016). Geological features and geochemical characteristics of late Devonian–early Carboniferous K-bentonites from northwestern Turkey. *Clay Minerals, 51*, 539–562.

Hastie, A. R., Kerr, A. C., Pearce, J. A., & Mitchell, S. F. (2007). Classification of altered volcanic island arc rocks using immobile trace elements: Development of the Th–Co discrimination diagram. *Journal of Petrology, 48*, 2341–2357.

Hayashi, K.-I., Fujisawa, H., Holland, H. D., & Ohmoto, H. (1997). Geochemistry of ~1.9 Ga sedimentary rocks from northeastern Labrador, Canada. *Geochimica et Cosmochimica Acta, 61*, 4115–4137.

He, B., Zhong, Y.-T., Xu, Y.-G., & Li, X.-H. (2014). Triggers of Permo-Triassic boundary mass extinction in south China: The Siberian traps or paleo-Tethys ignimbrite flare-up? *Lithos, 204*, 258–267.

Hetherington, C. J., Nakrem, H. A., & Potel, S. (2011). Note on the composition and mineralogy of Wenlock Silurian bentonites from the Ringerike district: Implications for local and regional stratigraphic correlation and sedimentary environments. *Norwegian Journal of Geology/Norsk Geologisk Tidsskrift, 91*, 181–192.

Hints, R., Kirsimäe, K., Somelar, P., Kallaste, T., & Kiipli, T. (2008). Multiphase Silurian bentonites in the Baltic palaeobasin. *Sedimentary Geology, 209*, 69–79.

Hodson, M. E. (2002). Experimental evidence for mobility of Zr and other trace elements in soils. *Geochimica et Cosmochimica Acta, 66*, 819–828.

Hong, H., Algeo, T. J., Fang, Q., Zhao, L., Ji, K., Yin, K., Wang, C., & Cheng, S. (2019). Facies dependence of the mineralogy and geochemistry of altered volcanic ash beds: An example from Permian-Triassic transition strata in southwestern China. *Earth-Science Reviews, 190*, 58–88.

Huff, W., Kolata, D., & Cross, T. (1989). Correlation of K-bentonite beds by chemical fingerprinting using multivariate statistics. In T. A. Cross (Ed.), *Quantitative Dynamic Stratigraphy* (pp. 567–577). New Jersey, USA: Prentice-Hall.

Huff, W., Merriman, R., Morgan, D., & Roberts, B. (1993). Distribution and tectonic setting of Ordovician K-bentonites in the United Kingdom. *Geological Magazine, 130*, 93–100.

Huff, W. D., Dronov, A. V., Sell, B., Kanygin, A. V., & Gonta, T. V. (2014). Traces of explosive volcanic eruptions in the Upper Ordovician of the Siberian platform. *Estonian Journal of Earth Sciences, 63*, 244–250.

Inanli, F. Ö., Huff, W. D., & Bergström, S. M. (2009). The Lower Silurian (Llandovery). Osmundsberg K-bentonite in Baltoscandia and the British Isles: Chemical fingerprinting and regional correlation. *GFF, 131*, 269–279.

Irvine, T., & Baragar, W. (1971). A guide to the chemical classification of the common volcanic rocks. *Canadian Journal of Earth Sciences, 8*, 523–548.

Kacmaz, H. (2016). Major, trace and rare earth element (REE). characteristics of tuffs in the Yenice-Saraycık area (Demirci, Manisa), western Anatolia, Turkey. *Journal of Geochemical Exploration, 168*, 169–176.

Kadir, S., Külah, T., Önalgil, N., Erkoyun, H., & Elliott, W. C. (2017). Mineralogy, geochemistry, and genesis of bentonites in Miocene volcanic-sedimentary units of the Ankara–Çankiri basin, central Anatolia, Turkey. *Clays and Clay Minerals, 65*, 64–91.

Khan, M. S. (1990). *Geochemical studies on the basal Aravalli (Lower Proterozoic). volcanic rocks around Udaipur, Rajasthan.* Aligarh Muslim University.

Kiipli, T., Kallaste, T., Nielsen, A. T., Schovsbo, N. H., & Siir, S. (2014). Geochemical discrimination of the Upper Ordovician Kinnekulle bentonite in the Billegrav-2 drill core section, Bornholm, denmark. *Estonian Journal of Earth Sciences, 63*, 264–270.

Kiipli, T., Hints, R., Kallaste, T., Verš, E., & Voolma, M. (2017). Immobile and mobile elements during the transition of volcanic ash to bentonite – an example from the early Palaeozoic sedimentary section of the Baltic basin. *Sedimentary Geology, 347*, 148–159.

Laviano, R., & Mongelli, G. (1996). Geochemistry and mineralogy as indicators of parental affinity for Cenozoic bentonites: A case study from S. Croce di Magliano (southern Apennines, Italy). *Clay Minerals, 31*, 391–401.

Liao, Z., Hu, W., Cao, J., Wang, X., Yao, S., Wu, H., & Wan, Y. (2016). Heterogeneous volcanism across the Permian–Triassic boundary in south China and implications for the latest Permian mass extinction: New evidence from volcanic ash layers in the lower Yangtze region. *Journal of Asian Earth Sciences, 127*, 197–210.

MacRae, N., Nesbitt, H., & Kronberg, B. (1992). Development of a positive Eu anomaly during diagenesis. *Earth and Planetary Science Letters, 109*, 585–591.

McDonough, W. F., & Sun, S.-S. (1995). The composition of the Earth. *Chemical Geology, 120*, 223–253.

McHenry, L. J. (2009). Element mobility during zeolitic and argillic alteration of volcanic ash in a closed-basin lacustrine environment: Case study Olduvai gorge, Tanzania. *Chemical Geology, 265*, 540–552.

McLennan, S. M. (1989). Rare earth elements in sedimentary rocks; influence of provenance and sedimentary processes. *Reviews in Mineralogy and Geochemistry, 21*, 169–200.

Merriman, R., & Roberts, B. (1990). Metabentonites in the Moffat shale group, Southern Uplands of Scotland: Geochemical evidence of ensialic marginal basin volcanism. *Geological Magazine, 127*, 259–271.

Modabberi, S., Namayandeh, A., López-Galindo, A., Viseras, C., Setti, M., & Ranjbaran, M. (2015). Characterization of Iranian bentonites to be used as pharmaceutical materials. *Applied Clay Science, 116–117*, 193–201.

Modabberi, S., Namayandeh, A., Setti, M., & López-Galindo, A. (2019). Genesis of the eastern Iranian bentonite deposits. *Applied Clay Science, 168*, 56–67.

https://doi.org/10.1007/s42860-019-00054-9 Published online by Cambridge University Press

Namayandeh, A., & Kabengi, N. (2019). Calorimetric study of the influence of aluminum substitution in ferrihydrite on sulfate adsorption and reversibility. *Journal of Colloid and Interface Science, 540*, 20–29.

Nath, B. N., Bau, M., Rao, B. R., & Rao, C. M. (1997). Trace and rare earth elemental variation in Arabian sea sediments through a transect across the oxygen minimum zone. *Geochimica et Cosmochimica Acta, 61*, 2375–2388.

Nesbitt, H. W. (1979). Mobility and fractionation of rare earth elements during weathering of a granodiorite. *Nature, 279*, 206.

Nesbitt, H. W., Markovics, G., & Price, R. C. (1980). Chemical processes affecting alkalis and alkaline earths during continental weathering. *Geochimica et Cosmochimica Acta, 44*, 1659–1666.

Özdamar, Ş., Ece, Ö. I., Uz, B., Boylu, F., Ercan, H. Ü., & Yanik, G. (2014). Element mobility during the formation of the Uzunisa-Ordu bentonite, NE Turkey, and potential applications. *Clay Minerals, 49*, 609–633.

Pang, K.-N., Chung, S.-L., Zarrinkoub, M. H., Mohammadi, S. S., Yang, H.-M., Chu, C.-H., Lee, H.-Y., & Lo, C.-H. (2012). Age, geochemical characteristics and petrogenesis of late Cenozoic intraplate alkali basalts in the Lut–Sistan region, eastern Iran. *Chemical Geology, 306–307*, 40–53.

Pang, K.-N., Chung, S.-L., Zarrinkoub, M. H., Khatib, M. M., Mohammadi, S. S., Chiu, H.-Y., Chu, C.-H., Lee, H.-Y., & Lo, C.-H. (2013). Eocene–Oligocene post-collisional magmatism in the Lut–Sistan region, eastern Iran: Magma genesis and tectonic implications. *Lithos, 180–181*, 234–251.

Pearce, J. A., Harris, N. B., & Tindle, A. G. (1984). Trace element discrimination diagrams for the tectonic interpretation of granitic rocks. *Journal of Petrology, 25*, 956–983.

Pellenard, P., Deconinck, J. F., Huff, W. D., Thierry, J., Marchand, D., Fortwengler, D., & Trouiller, A. (2003). Characterization and correlation of Upper Jurassic (Oxfordian). bentonite deposits in the Paris basin and the subAlpine basin, France. *Sedimentology, 50*, 1035–1060.

Renock, D., Landis, J. D., & Sharma, M. (2016). Reductive weathering of black shale and release of barium during hydraulic fracturing. *Applied Geochemistry, 65*, 73–86.

Rimstidt, J. D. (2014). *Geochemical Rate Models: An Introduction to Geochemical Kinetics*. Cambridge University Press.

Roberts, B., & Merriman, R. (1990). Cambrian and Ordovician metabentonites and their relevance to the origins of associated mudrocks in the northern sector of the Lower Palaeozoic Welsh marginal basin. *Geological Magazine, 127*, 31–43.

Schaefer, M. V., Guo, X., Gan, Y., Benner, S. G., Griffin, A. M., Gorski, C. A., Wang, Y., & Fendorf, S. (2017). Redox controls on arsenic enrichment and release from aquifer sediments in central Yangtze river basin. *Geochimica et Cosmochimica Acta, 204*, 104–119.

Siir, S., Kallaste, T., Kiipli, T., & Hints, R. (2015). Internal stratification of two thick Ordovician bentonites of Estonia: Deciphering primary magmatic, sedimentary, environmental and diagenetic signatures. *Estonian Journal of Earth Sciences, 64*, 140–158.

Slack, J. F., & Stevens, B. P. J. (1994). Clastic metasediments of the early Proterozoic Broken Hill group, New South Wales, Australia: Geochemistry, provenance, and metallogenic significance. *Geochimica et Cosmochimica Acta, 58*, 3633–3652.

Spears, D., & Kanaris-Sotiriou, R. (1979). A geochemical and mineralogical investigation of some British and other European tonsteins. *Sedimentology, 26*, 407–425.

Stocklin, J. (1968). Structural history and tectonics of Iran: A review. *AAPG Bulletin, 52*, 1229–1258.

Summa, L. L., & Verosub, K. L. (1992). Trace element mobility during early diagenesis of volcanic ash: Applications to stratigraphic correlation. *Quaternary International, 13–14*, 149–157.

Sverjensky, D. A. (1984). Europium redox equilibria in aqueous solution. *Earth and Planetary Science Letters, 67*, 70–78.

Voicu, G., & Bardoux, M. (2002). Geochemical behavior under tropical weathering of the Barama–Mazaruni greenstone belt at Omai gold mine, Guiana Shield. *Applied Geochemistry, 17*, 321–336.

Winchester, J., & Floyd, P. (1976). Geochemical magma type discrimination: Application to altered and metamorphosed basic igneous rocks. *Earth and Planetary Science Letters, 28*, 459–469.

Winchester, J. A., & Floyd, P. A. (1977). Geochemical discrimination of different magma series and their differentiation products using immobile elements. *Chemical Geology, 20*, 325–343.

Wray, D. S. (1995). Origin of clay-rich beds in Turonian chalks from Lower Saxony, Germany—a rare-earth element study. *Chemical Geology, 119*, 161–173.

Xing, L., Zhou, M., Qi, L., & Huang, Z. (2015). Discussion on the PGE anomalies and source materials of K-bentonite (Bed 5) in the Lower Cambrian Meishucun section, Yunnan. *Chinese Journal of Geochemistry, 34*, 346–361.

Yildiz, A., & Dumlupunar, I. (2009). Mineralogy and geochemical affinities of bentonites from Kapıkaya (Eskişehir, western Turkey). *Clay Minerals, 44*, 339–360.

Yildiz, A., & Kuscu, M. (2004). Origin of the basoren (Kutahya, W Turkey) bentonite deposits. *Clay Minerals, 39*, 219–231.

Yusoff, Z. M., Ngwenya, B. T., & Parsons, I. (2013). Mobility and fractionation of REEs during deep weathering of geochemically contrasting granites in a tropical setting, Malaysia. *Chemical Geology, 349*, 71–86.

Zhou, L., & Kyte, F. T. (1988). The Permian-Triassic boundary event: A geochemical study of three Chinese sections. *Earth and Planetary Science Letters, 90*, 411–421.

Zhou, Y., Bohor, B. F., & Ren, Y. (2000). Trace element geochemistry of altered volcanic ash layers (tonsteins). in late Permian coal-bearing formations of eastern Yunnan and western Guizhou provinces, China. *International Journal of Coal Geology, 44*, 305–324.

Zielinski, R. A. (1982). The mobility of uranium and other elements during alteration of rhyolite ash to montmorillonite: A case study in the Troublesome Formation, Colorado, U.S.A. *Chemical Geology, 35*, 185–204.

Zielinski, R. A. (1985). Element mobility during alteration of silicic ash to kaolinite—a study of tonstein. *Sedimentology, 32*, 567–579.

(Received 29 April 2019; revised 16 November 2019; AE: S. Kadir)

https://doi.org/10.1007/s42860-019-00054-9 Published online by Cambridge University Press